International Journal of Pediatric Otorhinolaryngology 101 (2017) 230–234

Contents lists available at ScienceDirect

International Journal of Pediatric Otorhinolaryngology

journal homepage: http://www.ijporlonline.com/

Anatomical measurement of the ossicles in patients with congenital aural atresia and stenosis

Jieying Li [a], Keguang Chen [a], Chenlong Li [a], Dongming Yin [a], Tianyu Zhang [a, b], Peidong Dai [a, b, *]

[a] ENT Institute, Eye & ENT Hospital of Fudan University, China
[b] Hearing Medicine Key Laboratory, National Health and Family Planning Commission, China

ARTICLE INFO

Article history:
Received 15 May 2017
Received in revised form
11 August 2017
Accepted 13 August 2017
Available online 18 August 2017

Keywords:
Ear ossicles
Computed tomography
Congenital aural stenosis
Congenital aural atresia

ABSTRACT

Objectives: Our aims were to measure and compare anatomical parameters of the ossicles in normal, congenital aural stenosis (CAS), and congenital aural atresia (CAA) ears.
Methods: This retrospective study was performed using three-dimensional reconstructed images derived from computed tomography scans of 20 normal subjects, 20 CAS patients, and 20 CAA patients.
Results: The lengths of the malleus handle and long process of the incus were greater in normal ears than in CAS and CAA ears (all $P < 0.05$). The angles of the incudostapedial joint and between the short and long processes of the incus were smaller in normal ears than in CAS and CAA ears (all $P < 0.05$). There were no significant differences in the positions of the malleus head and incudomalleolar joint, the size of the malleus head, the length of the short process of the incus, or the angle of the incudomalleolar joint ($P > 0.05$).
Conclusions: Anatomical parameters of the lower part, but not of the upper part, of the ossicular chain in CAS and CAA ears differed from those in normal ears. Different branchial arch origins of the upper and lower parts of the ossicular chain may explain these findings. Dysplasia of the second arch, which develops into the lower part of the ossicular chain, may contribute to ossicular malformation in CAA and CAS. Accurate radiographic measurement of malformed ossicles may be useful for reconstructive surgery of CAA and CAS using the patient's native ossicular chain and for choosing an appropriate place for active middle ear implants.

1. Introduction

Congenital dysplasia of the external and middle ear is frequently observed in neonates presenting at otology outpatient clinics, with an incidence ranging from 1 in 10,000 to 1 in 20,000 [1]. Its typical manifestations include microtia and variable malformation of the external auditory meatus. The number, size, and shape of the ossicles can be severely affected by this disorder [1]. The defect may impair the patient's quality of life, especially because it may hamper speech development in early life. Computed tomography (CT) is an established radiological technique that can reveal deformities of the external and middle ear, whereas magnetic resonance imaging (MRI) reveals the structures of the inner ear [1].

The ossicles develop from neural crest cells in the mesenchyme that migrate to the first and second branchial arches from the dorsal side of the neural tube in the fourth week of gestation [2,3]. After the cartilage primordium of each ossicle appears, the auditory ossicles start to develop at the foetal age of 5–7 weeks. There are two main theories regarding the role of each arch in ossicular development. The classical theory suggests that the malleus and the incus are derived from Meckel's cartilage in the first branchial arch. The second theory suggests that the upper part of the ossicular chain originates from the first arch and the lower part of the ossicular chain is derived from the second arch [4].

Developmental arrest and irregular embryogenesis caused by spontaneous genetic mutation may explain most cases of congenital dysplasia of the external and middle ear [5–7]. It has been suggested that deficient induction of the cartilage primordium in the early foetal stage can result in malformation of the auditory ossicles [8].

* Corresponding author. No.83 Fenyang Road, Shanghai 200031, China.
E-mail addresses: ljy777@126.com (J. Li), ckg19870715@163.com (K. Chen), chenlong.li@hotmail.com (C. Li), yindm90@163.com (D. Yin), ty.zhang2006@aliyun.com (T. Zhang), daipeidongent@163.com (P. Dai).

http://dx.doi.org/10.1016/j.ijporl.2017.08.013
0165-5876/© 2017 Published by Elsevier Ireland Ltd.

The aims of this study were to measure anatomical parameters of the ossicles in patients with congenital aural atresia (CAA), patients with congenital aural stenosis (CAS), and normal subjects, and to compare the anatomical parameters among these groups of subjects.

2. Materials and methods

2.1. Subjects

This study was approved by the ethics committee of our institution. This retrospective study was based on CT data obtained in patients diagnosed with microtia at our hospital between March 2009 and November 2015. Patients with disruption to or an absent ossicular chain and patients with cholesteatoma of the tympanic cavity were excluded from the study. CAS was diagnosed as a diameter of the external auditory canal of <4 mm, as proposed by Cole and Jahrsdoerfer. CAA was defined as total atresia of the external auditory canal and absence of the tympanic membrane.

The CAA group comprised 20 patients (16 males, 4 females) aged 5–23 years (median: 10 years). CAA was bilateral in 1 patient, affected the right ear in 13 patients, and affected the left ear in 6 patients. Therefore, the CAA group comprised 21 ears. The CAS group comprised 20 patients (7 females, 13 males) aged 4–17 years (median: 8 years). Stenosis affected the right ear in 14 patients and the left ear in 6 patients. Therefore, the CAS group comprised 20 ears. The control group comprised 20 patients (17 males, 3 females) aged 7–24 years (median: 10 years) who were randomly selected from outpatients with radiological normal temporal bone CT images. The right ear was measured in 4 subjects and the left ear was measured in 16 subjects. There were no differences in age or gender among the three groups.

2.2. Data acquisition and post-processing

All digital imaging and communication in medicine (DICOM) images were obtained with a multi-detector row CT unit (Sensation 16; Siemens Medical Systems, Forchheim, Germany) operating in helical mode. The tube voltage was 120 kVp and the tube current was 180 mA. All images were obtained using a standard temporal bone protocol. Regarding image resolution, the thickness of each slice was 0.75 mm with a 0.5 mm increment per slice, a 512 × 512 matrix, and pixel size of 0.43 mm. The display field-of-view of each slice was 22.0 × 22.0 cm. The window centre and width were 700 and 4000 HU, respectively.

The two-dimensional DICOM data were exported to Mimics 12.1 software (Materialize, Brussels, Belgium) for processing into three-dimensional images [9] using a contrast scale range of 1024–2000 HU; these values represent air and bone, respectively.

2.3. Calculations

Bone landmarks were identified as illustrated in Fig. 1, for all subjects. The following landmarks were confirmed by three-dimensional reconstruction: the central points of the malleus head (M_{head}), malleus neck (M_{neck}), and incudomalleolar joint ($J_{inc-mal}$); the distal ends of the long process of the incus (Inc_l), the short process of the incus (Inc_{sh}), and the malleus handle (M_{handle}); the upper point of the malleus head (M_{up}); the anterior point of the stapes footplate (Ft_{ant}); the posterior point of the stapes footplate (Ft_{post}); the midpoint of the superior border of the stapes footplate (Ft_{sup}); and the midpoint of the inferior border of the stapes footplate (Ft_{inf}).

To accurately determine the positions of the malleus head and the incudomalleolar joint, a standard three-dimensional coordinate system was used, based on the Frankfurt horizontal plane (Pfrkt) and two perpendicular planes [10]. Pfrkt was defined as the plane passing through the point of the left orbitale and the superior margins of the bilateral external auditory canals. The median sagittal plane (Psag) was defined as the plane passing through the top of the crista galli and the midpoint of the line connecting the tips of the bilateral posterior clinoid processes. The Psag and the Pfrkt are perpendicular to each other. The coronal plane (Pcor) was defined as the plane passing through the midpoint of the line linking the tips of the bilateral posterior clinoid processes and is perpendicular to each of the Pfrkt and the Psag. The position of the malleus head was defined as the distance between M_{head} and each of the Pfrkt, Psag, and Pcor. The position of the incudomalleolar joint was defined as the distance between the point $J_{inc-mal}$ and each of the Pfrkt, Psag, and Pcor (see Table 1).

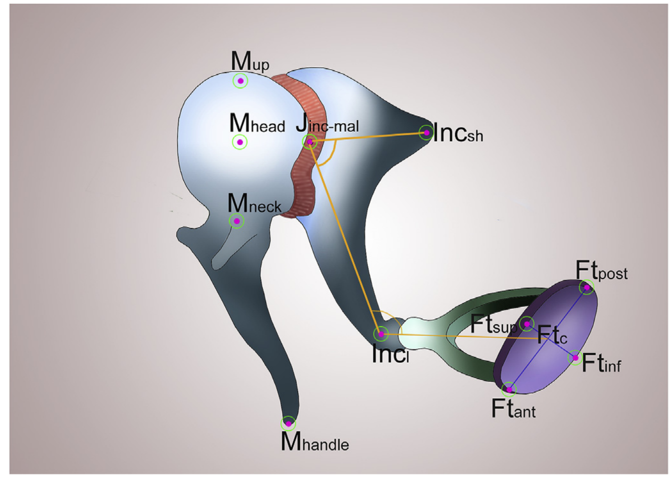

Fig. 1. Schematic diagram of the ossicles showing the following landmarks: the central points of the malleus head (M_{head}), the malleus neck (M_{neck}), and the incudomalleolar joint ($J_{inc-mal}$); the distal ends of the long process of the incus (Inc_l), the short process of the incus (Inc_{sh}), and the malleus handle (M_{handle}); the upper point of the malleus head (M_{up}); the anterior point of the stapes footplate (Ft_{ant}); the posterior point of the stapes footplate (Ft_{post}); the midpoint of the superior border of the stapes footplate (Ft_{sup}); the midpoint of the inferior borders of the stapes footplate (Ft_{inf}); and the central point of the stapes footplate (Ft_c). The diagram also shows the angle between the short and long processes of the incus ($\angle Inc_{sh}\ J_{inc-mal}\ Inc_l$) and the angle of the incudo-stapedial joint ($\angle J_{inc-mal}\ Inc_l Ft_c$).

The length of the malleus handle was defined as the distance from M_{neck} to M_{handle}. The lengths of the short and long processes of the incus were defined as the distances from $J_{inc-mal}$ to Inc_{sh} and to Inc_l, respectively. The superior, inferior and posterior radii of the malleus head were defined as the radii from M_{head} to M_{up}, M_{neck}, and $J_{inc-mal}$, respectively. The angle between the short and long processes of the incus ($\angle Inc_{sh}\ J_{inc-mal}\ Inc_l$) was defined as the angle between the line from $J_{inc-mal}$ to Inc_{sh} and the line from $J_{incu-mal}$ to Inc_l. The centre of the stapes footplate (Ft_c) was defined as the intersection of the line passing from Ft_{ant} to Ft_{post} and the line passing from Ft_{sup} to Ft_{inf}. The angle of the incudostapedial joint ($\angle J_{inc-mal}\ Inc_l Ft_c$) was defined as the angle between the line from Inc_l to $J_{incu-mal}$ and the line from Inc_l to Ft_c. The angle of the incudomalleolar joint was defined as the angle between the line from $J_{inc-mal}$ to M_{head} and the line from $J_{inc-mal}$ to Inc_{sh} ($\angle M_{head}\ J_{inc-mal}\ Inc_{sh}$). All measurements were taken by one author (Li) using Mimics 12.1 software. The landmarks were determined using predefined standards on the three-dimensional reconstructed images. The three-dimensional coordinates for each landmark were entered into the OssicleCalculation application written in Matlab (Mathworks, Cambridge, UK) to calculate the point-to-point distances, point-to-plane distances, and angles between lines.